

# Characteristics of an Additively Manufactured Titanium Oscillating Heat Pipe

Michael Cox<sup>1</sup> and Takuro Daimaru<sup>2</sup>

*Jet Propulsion Laboratory, California Institute of Technology, Pasadena, CA 91109*

Isothermalization of spacecraft structures is often necessary for JPL's science missions. Oscillating heat pipes (OHPs) are compact devices that utilize latent heat to passively isothermalize a surface with tremendous effect. These OHP channels can be embedded within a structure of any geometry with additive manufacturing to significantly increase the effective conductivity of the material. OHPs have previously been made with aluminum to maximize heat transfer capability but OHPs can also greatly enhance materials such as titanium with poor thermal conduction. In spacecraft design, titanium is a desirable material due to its structural strength, but is often not used in key thermal infrastructure due to its low conductivity unless thermal isolation is required. Therefore, isothermalizing materials that have previously been disqualified from design applications due to poor thermal performance opens up new possibilities for efficient design. As a result, a novel additively manufactured titanium OHP has been developed to characterize the performance of OHP technology within low-conducting materials. The prototype OHP is embedded in a flat plate sample as a monolithic piece, thus removing any internal interface resistances, with 42 turns and a working fluid of R-134a as is consistent with other material OHP tests. Furthermore, the prototype shows a two-orders of magnitude increase in thermal conductivity compared to normal titanium. This study demonstrates the design, manufacturing, and thermal performance characteristics of the prototype titanium OHP and its potential for thermal design moving forward.

## Nomenclature

<i>OHP</i>	=	oscillating heat pipe
<i>TiOHP</i>	=	titanium (Ti-6Al-4V) oscillating heat pipe
<i>AM</i>	=	additively manufacture
<i>A</i>	=	cross-section area
<i>L</i>	=	length
<i>G</i>	=	conductance
<i>k</i>	=	conductivity
<i>T</i>	=	temperature
$q_{HTR}$	=	heater thermal power into system
<i>eff</i>	=	denotes effective property
<i>evap</i>	=	denotes for evaporator region
<i>cond</i>	=	denotes for condenser region
<i>adiabatic</i>	=	denotes for adiabatic region

---

<sup>1</sup> Thermal Engineer, Propulsion, Thermal, and Materials Engineering, 4800 Oak Grove Dr., Pasadena, CA 91109, Mail Stop 125-109.

<sup>2</sup> Thermal Technologist, Propulsion, Thermal, and Materials Engineering, 4800 Oak Grove Dr., Pasadena, CA 91109, Mail Stop 125-109.

## I. Introduction

IN spacecraft applications, maximizing the efficiency of thermal and mechanical structures is paramount to the success of a mission and the ability to survive the extremes of the surrounding environments. For most spacecraft, structures must serve the design by either isolating or coupling different areas of the spacecraft<sup>1</sup>. Currently, these thermal designs are driven by material choice and geometry. High conductive structures must have a high material conductivity coupled with a high cross section area per length (A/L) ratio. Conversely, isolative structures must have the opposite, meaning low thermal conductivity and minimization of the A/L ratio<sup>1</sup>. Furthermore, these thermal requirements restrict the mechanical design of structures and often result in heavier and less efficient mass designs. Thus, utilizing these oscillating heat pipes (OHPs) creates a design free from this restriction that improves the benefit of both thermal and mechanical design.

## II. Background

OHPs are passive two-phase fluid-gas systems created by Akachi<sup>2</sup> that utilize latent heat and capillary flow to conduct large amounts of heat with little temperature change all with the simplicity of a single small wick-less tube<sup>3</sup>.

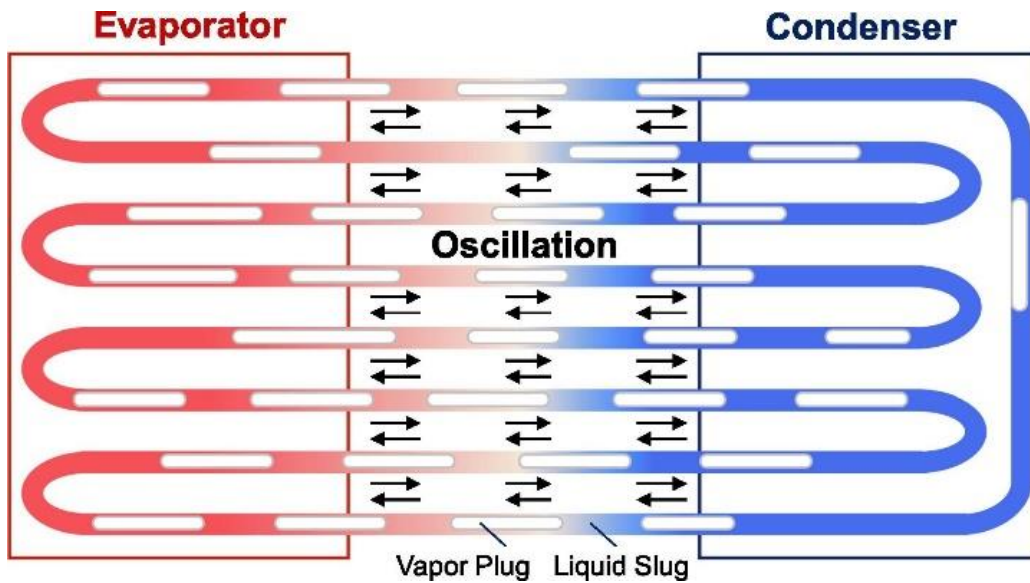
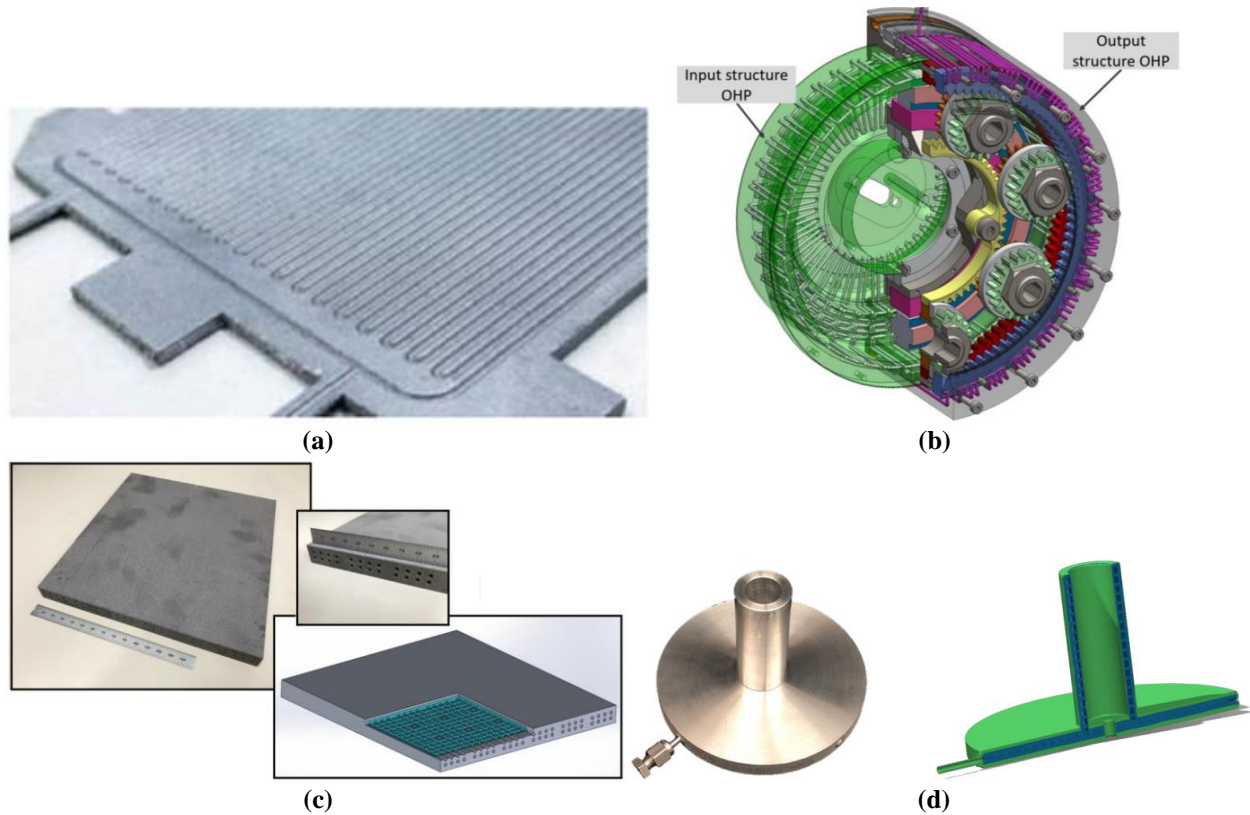


Figure 1. Graphic Representation of OHP Schematic and liquid-vapor slug oscillation<sup>4</sup>

This simple OHP tube can easily be embedded into a structural design with laser-sintering additive manufacturing (AM) to allow seamless heat transfer without any additional interfaces<sup>5</sup>. At JPL, AM OHP designs have already been developed using an aluminum alloy (AlSi10Mg) as a host material<sup>6</sup> and have shown an ~39 times increase in thermal conductivity performance compared to solid AlSi10Mg<sup>4</sup>.



**Figure 2. AM OHP Designs Developed at JPL a) Aluminum AM OHP flat plate<sup>4</sup>, b) AM OHP embedded electric actuator<sup>7</sup>, c) AM porous evaporator<sup>8</sup>, d) AM heat pipe embedded Li-ion battery case<sup>9</sup>**

Now an iteration of the successful AMOHP flat plate design has been developed with titanium (Ti-6Al-4V) as a host material to study the effects of material selection in the design and viability of titanium OHPs for future design capability. While having a high conductivity does help with OHP performance, compared to the latent heat of the liquid-vapor process, it is a second order effect<sup>10</sup>. Although most OHP designs have been high conductivity materials such as copper and aluminum<sup>10</sup> changing the material of the OHP to a low conductivity material expands the use of OHPs to not just the conventional high conductivity materials but materials of other advantageous properties previously not even considered for thermal design due to their low conductivity.

### III. Experimental Setup

The flat plate TiOHP prototype geometry and testing procedure is a replication of previous aluminum AM OHP prototypes developed by JPL in which design performance is measured from temperature deltas across the plate for a given heater input. Figure 3 shows the flat plate prototype design and testing method. Table 1 shows the OHP design characteristics and a comparison to previous aluminum OHP testing.

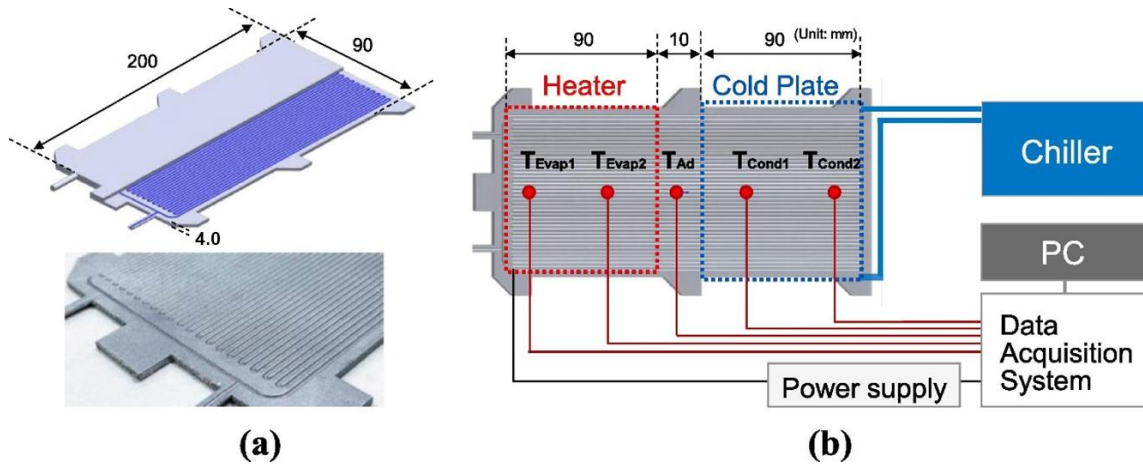


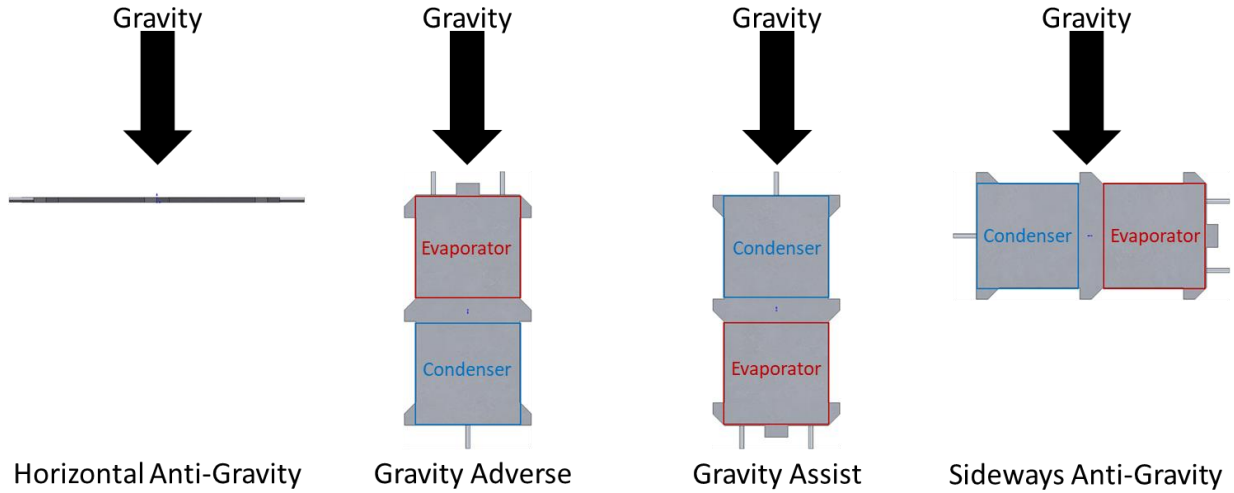
Figure 3. a) AM OHP Dimensions and channel geometry, b) Performance test set-up and TC locations<sup>4</sup>

Table 1. OHP Design Characteristics

OHP Material	Ti-6Al-4V	AlSi10Mg <sup>4</sup>
Material Conductivity, W/m-K	6.7 <sup>6</sup>	160
Inner channel diameter, mm	1.0	1.0
Radius of turns, mm	1.0	1.0
Number of turns	42	42
Total channel length, mm	7944	7944
Width of OHP, mm	90	90
Length of OHP, mm	200	200
Thickness of OHP, mm	4.0	3.8
Working fluid	R134a	R134a
Charge ratio, wt%	53	45

During testing, the evaporator section of the prototype was heated by a Kapton heater and a DC power source (Xantrex XFR 300-4) that would output heat loads up to 130 W into the system. The condenser section was pressure mounted with clamps and a thermal interface material to a cold plate with an integrated chiller and an inlet temperature of 10 C. In order to reduce environmental losses during the experiment, the test set up was wrapped in thermal insulation. Temperatures were measured using E Type thermocouples connected to a data logger (Keysight DAQ970A).

In order to capture the gravity effects on the OHP performance, tests were conducted in horizontal (anti-gravity) configuration, vertical evaporator side up (gravity-adverse), vertical evaporator down (gravity assisting), and sideways (gravity only at turns).



**Figure 4. Testing Configurations with respect to Gravity**

The first orientation tested, the horizontal anti-gravity orientation was tested 3 times in order to capture experimental uncertainty. However, due to the repeatability seen by the OHP performance, the remaining orientations were tested once with an assumed uncertainty similar to the horizontal anti-gravity case. Furthermore, the overall conductance and conductivity of the design was found for each orientation using equations 1 and 2. While adiabatic length used for conductivity calculation is often taken as the free length between the evaporator and condenser sections<sup>11</sup>, in accordance with previous testing, the adiabatic length was taken from the center of the condenser section to the center of the evaporator section (100 mm)<sup>4</sup> in order to have direct comparison.

$$G_{eff} = \frac{q_{HTR}}{T_{evap} - T_{cond}} \quad (1)$$

$$k_{eff} = \frac{L_{adiabatic}}{A} * \frac{q_{HTR}}{T_{evap} - T_{cond}} \quad (2)$$

#### IV. Results

##### Ti OHP Steady State Analysis Gravity Assist-Evap on Bottom

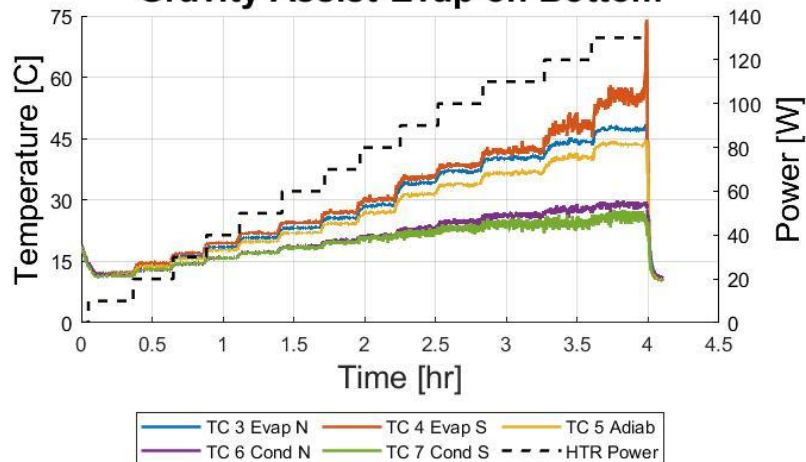


**Figure 5. Temperature Data of Gravity-Assist Orientation Steady State Test**

The temperature data from the experiments was captured until steady state was achieved at each heater power level. The temperature vs power plots for the remaining orientations can be found in the appendix. This steady state temperature data was then used to determine the thermal conductive performance of the TiOHP using equations 1 and 2 for the various different gravity orientations.

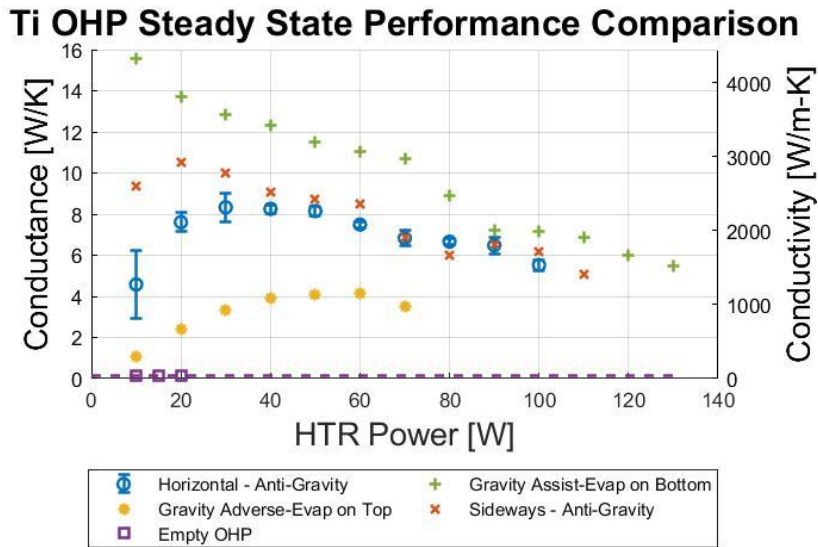


**Figure 6. Steady State Conductance and Conductivity Results for Ti OHP**

**Table 2. Comparison of Ti-6Al-4V and AlSi10Mg OHP Performance**

Performance	Ti-6Al-4V (Anti-Gravity Horizontal)	AlSi10Mg (Anti-Gravity Horizontal) <sup>4</sup>
Peak Eff. Conductivity, W/m-K	2315	6262
Heater Power at Peak Performance, W	30	20
Dry Out Power, W	100	>200 (Test did not reach dry out)
Empty-Channel Eff. Conductivity, W/m-K	6.1	145
Solid Material Conductivity, W/m-K	6.7	160
Improvement Factor, [OHP]/[Solid]	346	39

The TiOHP design testing reveals that using additive manufacturing to embed OHPs in Ti-6Al-4V in a neutral orientation increases peak conductance and conductivity by over 340 times the bare titanium equivalent design. This improvement factor is nearly 9 times greater than the improvement factor for embedded aluminum OHP. The large increase observed is due to the proportional impact of the two-phase heat transfer within the channels compared to the host material. Since the conductivity of OHP channels is so high, it drives the effective conductivity. Similarly, because the conductivity of the channels is so high, the host material conductivity's impact on the effective conductivity is reduced meaning low conductivity host materials show a higher improvement factor<sup>4</sup>.

**Table 3. Gravity Orientation Peak Performance Comparison**

Orientation	Peak Conductivity, W/m-K	Dry-Out Power, W
Anti-Gravity – Horizontal	2315	100
Gravity Assist – Evap. Down	4325	130
Gravity Adverse – Evap. Up	1150	90
Anti-Gravity – Sideways	2921	110

The best performing orientation in both peak conductance/conductivity and operating range before dry-out was found to be the vertical evaporator down gravity-assisting orientation. In this orientation, the TiOHP peaks in performance in low power modes and gradually declines in performance before drying out at 130 W. In addition, at this peak performance, the TiOHP performs over 645 times better than bare titanium. Even right before dry out,



despite the performance loss, this orientation is still 227 times more conductive than bare titanium and 10 times more conductive than bare aluminum. It should be noted that this trend of peak conductivity followed by reduced performance before dry-out is different from other OHP testing with more conventional manufacturing techniques where performance increases with increasing power without a drop-off. However, this trend seen in this study is in agreement with other additively manufactured OHPs produced at JPL. It is suspected that this difference may be caused by the surface roughness of additively manufactured internal channels which are not smoothed after printing. However, this is a trend that requires further examination.

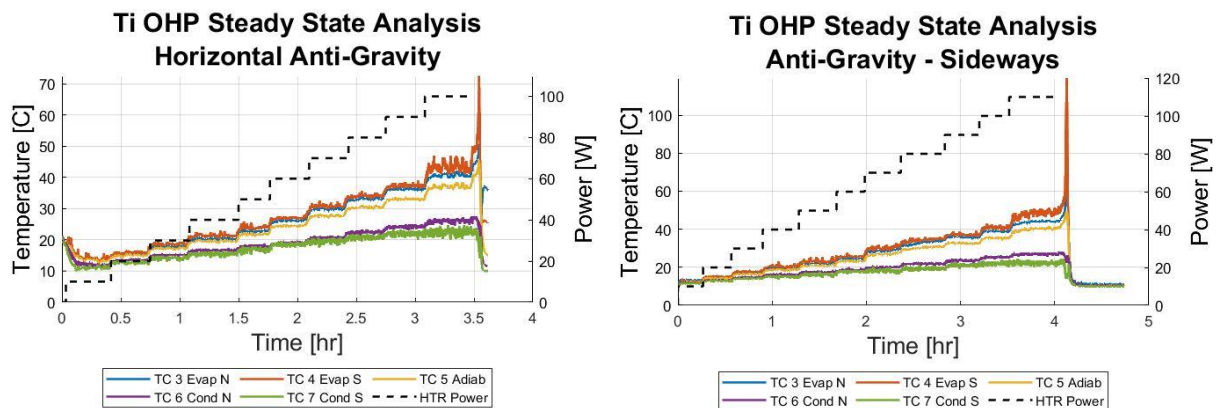
Conversely, the worst performing orientation was found to be the vertical evaporator up gravity-adverse orientation which had both the lowest peak conductive performance as well as the smallest operating range of powers. Despite this, the TiOHP in this worst case orientation still operated up to 172 times better than bare titanium and 7 times better than bare aluminum of the same geometry.

Another observation seen is that the sideways anti-gravity orientation performs slightly better in lower powers than the horizontal anti-gravity orientation. This is suspected due to the gravity at turns assisting start up to happen quicker for lower powers for the sideways orientation. In comparison, the horizontal orientation has little gravity assistance to overcome the capillary pressure required to move the liquid slug around the turn thus delaying start up for lower powers.

## V. Conclusions and Future Work

The performance of the additively manufactured Ti-6Al-4V oscillating heat pipe shows at best an over 645 times increase in peak thermal conductivity from un-modified Ti-6Al-4V material and a 27 times increase in peak performance over aluminum (AlSi10Mg). This peak occurs in the gravity assist (evaporator down) orientation which increases peak performance by 2010 W/m-K over the neutral horizontal orientation. Conversely, the gravity adverse (evaporator up) orientation decreases peak performance by 1165 W/m-K compared to the neutral orientation but still increases thermal performance by two orders of magnitude over solid Ti-6Al-4V. With this increase in effective thermal conductivity, TiOHPs incorporate the mechanical strength benefits of titanium all while exceeding thermal performance of high conductivity materials such as aluminum and copper. This duality significantly opens the thermal-mechanical design space for space applications where mechanical and thermal needs for material selection are no longer contradictory. With embedded OHPs, even low conductivity materials like titanium or other materials that have previously been written off for poor thermal performance can now be improved to high conductivity structures. This also opens the door for a multitude of future work at JPL including testing more host materials to further understand compatibility and performance increase, embedding TiOHPs in more complex geometries to expand the scope of OHP usage, and developing TiOHP heat switches to take advantage of low off-conductance host titanium and high conductance OHPs.

## Appendix



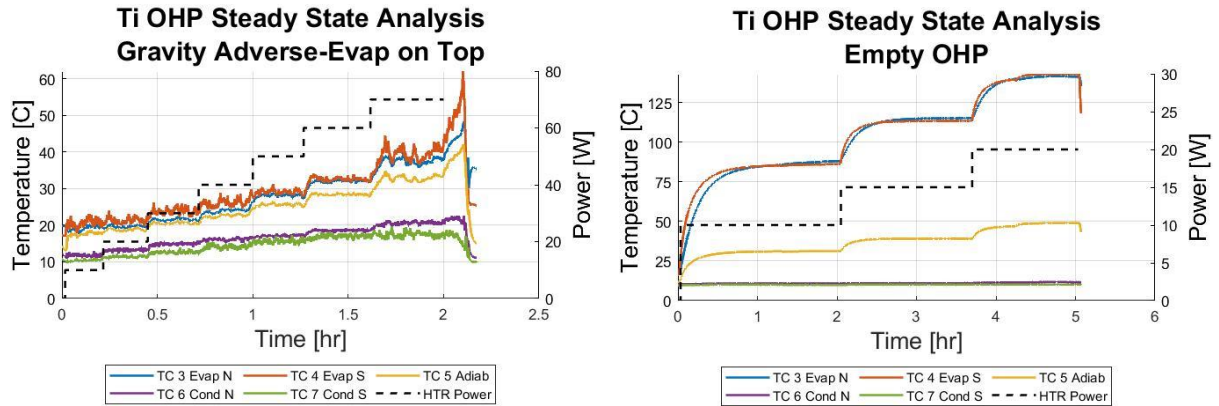


**Figure 7. Temperature Data for Steady State Testing at various Gravity Orientations**

### Acknowledgments

This research was carried out at the Jet Propulsion Laboratory, California Institute of Technology, USA under internal research and technology development funding under contract with NASA.

### References

- <sup>1</sup>D. Gilmore. "Spacecraft Thermal Control Handbook." *American Institute of Aeronautics and Astronautics*, 2002
- <sup>2</sup>H. Akachi, U.S. Patent, Patent Number 4921041, May 1, 1990.
- <sup>3</sup>S.P. Das et al. "Thermally induced two-phase oscillating flow inside a capillary tube." *International Journal of Heat and Mass Transfer*, Vol. 53, Issues 19-20, 2010.
- <sup>4</sup>K. Odagiri et al. "Three-dimensional heat transfer analysis of flat-plate oscillating heat pipes." *Applied Thermal Engineering*, Vol. 195, 2021.
- <sup>5</sup>B. Richard, D. Pellicone, B. Anderson. "Loop Heat Pipe Wick Fabrication via Additive Manufacturing." *48th International Conference on Environmental Systems*, 2018.
- <sup>6</sup>R. Gotoh et al. "Experimental and analytical investigations of AlSi10Mg, stainless steel, Inconel 625, and Ti-6Al-4V porous materials printed via powder bed fusion." *Progress in Additive Manufacturing*, Vol. 7, 2022.
- <sup>7</sup>E. Maghsoudi et al. "Efficient Thermal Management for Sampling Arm Actuators." *50th International Conference on Environmental Systems*, 2020.
- <sup>8</sup>B. Furst et al. "An Additively Manufactured Evaporator with Integrated Porous Structures for Two-Phase Thermal Control." *48th International Conference on Environmental Systems*, 2018.
- <sup>9</sup>B. Furst, R. Bugga, S. Roberts. "A Concept Demonstrator for an Additively Manufactured Li-ion Battery Case with Embedded Heat Pipes." *50th International Conference on Environmental Systems*, 2020.
- <sup>10</sup>D. Bastakoti et al. "An overview on the developing trend of pulsating heat pipe and its performance." *Applied Thermal Engineering*, Vol. 141, 2018.
- <sup>11</sup>W. Witts et al. "Experimental Investigation of a Flat-Plate Closed-Loop Pulsating Heat Pipe." *ASME Journal of Heat and Mass Transfer*, Vol. 141, 2019